Journal of Zankoy Sulaimani
Part-A- (Pure and Applied Sciences)
http://jzs.univsul.edu.iq

Throughput Performance Evaluation of LTE-Advanced with Inter-band Carrier Aggregation

Salim Qadir Mohammed[1*] & Dana Salahalddin Abdalla [1]

[1] *Technical College of Engineering- Sulaimani Polytechnic University, Sulaimani, Kurdistan Region- Iraq*
**Corresponding author's e-mail: salim.muhammed@spu.edu.iq*

Article info

Original: 6 October 2017
Revised: 27 August 2019
Accepted:17 November 2019
Published online: 20 June 2020

Key Words:
LTE-Advanced, Carrier Aggregation, ITU, Link Level Simulation, Throughput.

Abstract

The increasing number of mobile smartphone users requires additional spectrum to maintain cellular quality of service. The 800 MHz band is a good candidate to achieve this goal. It can be used as standalone spectrum or aggregated with other licensed bands to increase the available bandwidth. This paper compares through physical layer simulation the downlink throughput versus distance performance of LTE-Advanced in two different bands. We consider a high frequency band at 2.6 GHz and the 800 MHz to model bands 7 and 20 of inter-band carrier aggregation CA_7-20 respectively. The link level simulation is performed for single antenna system at three different urban locations. The channel is modelled using an enhanced 3D ITU-R channel model combined with measured 3D radiation patterns for the base station and user equipment antennas. The BER versus SNR results show that the 800 MHz band enjoys a gain of up to 1 dB as a result of higher Ricean K-factors. Moreover, for the assumed simulation parameters, at distances beyond 400 m the throughput of the 800 MHz band is significantly higher than the 2.6 GHz band. At a distance of 750 m, the throughput for the 800 MHz band is 4.5 times greater than the 2.6 GHz band. These benefits are shown to relate to the lower path loss values observed in the 800 MHz band.

Introduction

Over the last 25 years the internet has become a powerful tool that provides numerous services to its users. The target of 2G and 3G mobile operators is to support voice and IP services to a wide range of mobile devices. Recent capacity demands have led to the evolution of 3G to LTE and LTE-Advanced (4G). Bandwidth flexibility (from 1.4 MHz to 20 MHz) is one of the main characteristics of LTE. This allows radio access deployment in different frequency bands, each having unique characteristics [1]. Even with using the 20 MHz bandwidth it is not possible to achieve the target maximum data rate in LTE-Advanced (1 Gbps in the downlink and 500 Mbps in the uplink, compared with 100 Mbps in the downlink and 50 Mbps in the uplink for LTE). Hence there is a need to identify additional spectrum. Therefore, carrier aggregation (CA) up to five times the standard LTE bandwidth is supported by the standard. This feature enables terminals to exploit intra and/or inter band fragmented spectrum. Figure-1 shows the downlink peak data rate versus the year of their commercial availability for different mobile communication technologies. These technologies are known as releases in the 3GPP specifications [2].

The 3GPP Release 11 of LTE-Advanced includes requirements of inter-band carrier aggregation. Carrier aggregation is easier to implement at the Base Station (BS) rather than the User Equipment (UE). The BS uses different Radio Frequency (RF) modules for different bands. Current wide band antennas support operating frequencies in the range 1.8-2.6 GHz and separate antennas are required for frequencies below 1GHz. UE uses four categories to combine between bands [3].

Recent researches have explored how best to access additional spectrum. A number of studies have focused on the use of unlicensed 60 GHz bands. Although at these frequencies large amounts of new spectrum are available, propagation path loss is extreme [4]. Utilizing the unused licensed VHF and UHF bands of Digital Terrestrial Television (DTT), which are known as TV White Space, is another method to

increase spectrum. The RF propagation performance in the TV white space bands (below 800 MHz) is much better than the higher frequency cellular bands commonly in use today ***[5]***.

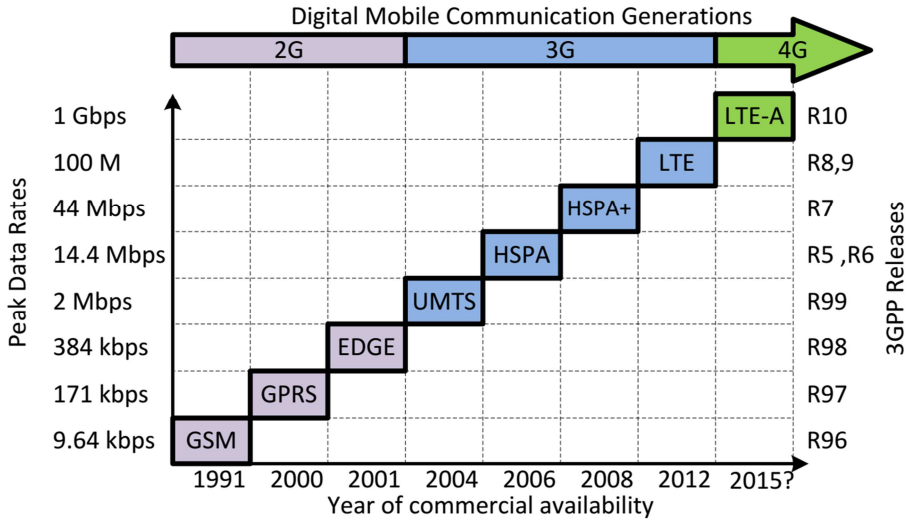

Figure-1: Peak data rates of different mobile communication technologies [2].

In this paper, the LTE-Advanced link level simulator of [6] is used to obtain the Packet Error rate (PER) and downlink throughput for a number of urban users. An enhanced 3D ITU-R channel modelling tool is used to model the channel in urban environment at carrier frequencies of 800 MHz and 2.6 GHz. The remainder of this paper is organized as follows. The following sub-sections provide information relating to LTE-Advanced, carrier aggregation, and the enhanced 3D ITU-R channel model. The Simulation Results section presents the physical layer PER and throughput results of the LTE-Advanced, and finally conclusions are drawn in the Conclusion section.

A. LTE-Advanced

OFDM is the basic transmission scheme for the downlink of LTE-Advanced. The selection of the OFDM parameters depends on the E-UTRA transmission bandwidth which can be any of the following values: 1.4, 3, 5, 10, 15 or 20 MHz [7]. The subcarrier spacing is the same for all supported bandwidths. Table-1 summarizes the OFDM parameters. Figure-2 shows the block diagram of the LTE transmitter. It consists of two main parts, 1) transport channel processing and 2) physical channel processing. The reverse operations are performed at the receiver.

Table-1: Downlink Simulation Parameters

Parameters	**Value**
System Bandwidth (MHz)	10
Subcarrier Spacing (kHz)	15
Sampling Frequency (MHz)	15.36
FFT size	1024
Occupied Subcarriers	600
CP length (samples)	72
Number of Codewords	1
Number of Code Block	1
Coding	Turbo Coding (1/3),

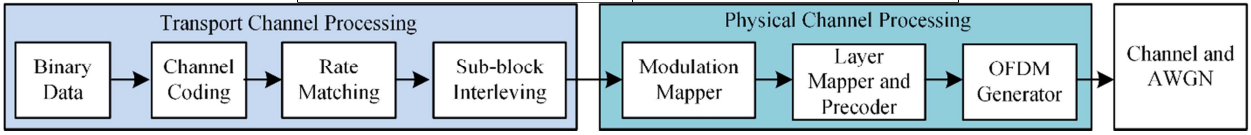

Figure-2: Block diagram of the downlink LTE transmitter

B. Carrier Aggregation

According to the IMT-Advanced requirements, LTE-Advanced aims to achieve a peak downlink data rate of 1 Gbps and an average spectrum efficiency of 3.7 bps/Hz/cell, which in turns requires more spectrum [7]. Wider bandwidths of up to 100 MHz are possible in the LTE-Advanced standard through the aggregation of several contiguous or non-contiguous fragmented spectrum. Figure-3 shows different scenarios for carrier aggregation. The inter-band aggregation between high and low frequencies (case c) is considered in this study. Operation in the high-low combination is more complex at the UE. Table-2 shows the CA operation bands for uplink and downlink as planned in Release 11 of the LTE-Advanced standard.

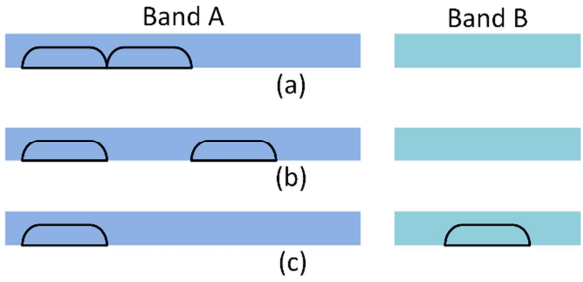

Figure-3: Possible Carrier Aggregation Scenarios [1]; (a) Contiguous Intra-band, (b) Non- Contiguous Intra-band, (c) Inter-band

Table-2: Inter-Band CA Operating Bands ***[3]***

E-UTRA CA Band	**E-UTRA Band**	**Operating Band in MHz**	
		Uplink	***Downlink***
CA_1-5	1	1920 – 1980	2110 – 2170
	5	824 – 849	869 – 894
CA_4-13	4	1710 – 1755	2110 – 2155
	13	777 – 787	746 – 756
CA_7-20	7	2500 – 2570	2620 – 2690
	20	832 – 862	791 – 821
CA_2-17	2	1850 – 1910	1930 – 1990
	17	704 – 716	734 – 746
CA_3-20	3	1710 – 1785	1805 – 1880
	20	832 – 862	791 – 821

C. Channel Model

The communication channels in this paper are generated using the enhanced 3D international telecommunication union-radio communication sector (ITU-R) channel model [8]. The ITU-R model is a geometry based stochastic channel model (GSCM) with various levels of randomness to model different BS-UE links. As shown in Figure-4, the channel generation process for the enhanced 3D ITU-R GSCM [9] can be summarized in six steps. These are classified into three phases: 1) UE parameters, 2) generation of LSP propagation parameter and 3) generation of channel impulse response. The user parameter part (step1) is used to setup simulation parameters, such as the type of environment, the numbers of BSs and UEs, the directions and speeds of the UE. In this phase, the users also can supply the antenna at both the BS and UE, the spacing and orientations of the antenna elements.

The second part of the channel creation process is the propagation parameter generation, which consists of path loss (PL), shadow fading (SF) calculation and the generation of the large-scale parameters (LSPs) and small-scale parameters (SSPs) for the channel. LSPs are generated based on a pre-defined Probability Distribution Function (PDF) with specific mean and standard deviation. These include the Root Mean Square (RMS) delay spread (DS), the RMS Angle of Arrival (AoA) and Angle of Departure (AoD) in both azimuth and elevation planes, the K-Factor and the SF. The de-correlation distances and cross correlations are calculated for the generated LSPs. For more details on these parameters please refer to [10].

The SSPs are generated based on the LSPs from step 3. The SSPs represent the information associated with each multipath component (MPC). This include the phase, delay, angular information for each individual cluster and ray within the cluster. This is performed based on the predefined PDFs. Step 5 represents the generation of the channel impulse response (time domain). This includes generating random phases for the rays within cluster and apply the cross-polarization effect between antenna elements. Then the Doppler effect is added in case of mobility. Finally, in step 6, PL and SF values are applied to the channel impulse responses. This stage enables system level studies to be performed. An open source code of the enhanced 3D ITU-R channel model is available at [11].

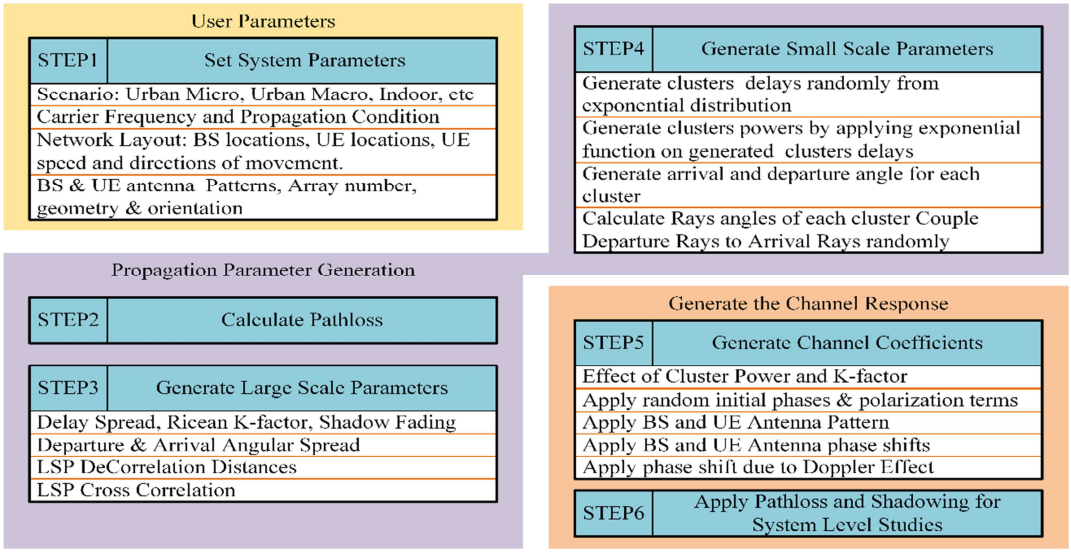

Figure-4: Enhanced 3D ITU-R channel modeling process

Using the enhanced 3D ITU-R channel, Many UEs were deployed randomly over a hexagonal area with a radius of 1000 m within a 120^{o} sector, a macro-cell base station antenna height of 30 m, and base station transmit power of 43 dBm. Each user was modelled at 1.5 m above ground level. The system was modelled at 800 MHz and 2.6 GHz using a 13.8 dBi directional antenna down-tilted by 10^{o} at the BS side and an omni-directional antenna with a maximum directivity of 6.8 dBi at the UE side.

Figure-5 shows the total average received signal strengths at different UE locations as a function of the distance from the BS for the two frequency bands. It can be seen that the 800 MHz band offers considerably higher RF signal levels. The solid red and blue lines represent best fit models corresponding to the 800 MHz and 2.6 GHz bands respectively. For the remaining analysis three specific UE locations were chosen. Table-3 presents the distance from the base station, the RMS DS, the K-factor, and the carrier frequency for each of these UE locations.

Table-3: Propagation Characteristics of The Six Different Studied Links

Scenario	**BS-UE Distance (m)**	**RMS DS (ns)**	**K-factor (dB)**	**Carrier frequency (MHz)**
S1a	100	95	9	800
S2a	800	692	-5.71	
S3a	900	129.3	14.85	
S1b	100	162	7.6	2600
S2b	800	663	-1.62	
S3b	900	358	7.37	

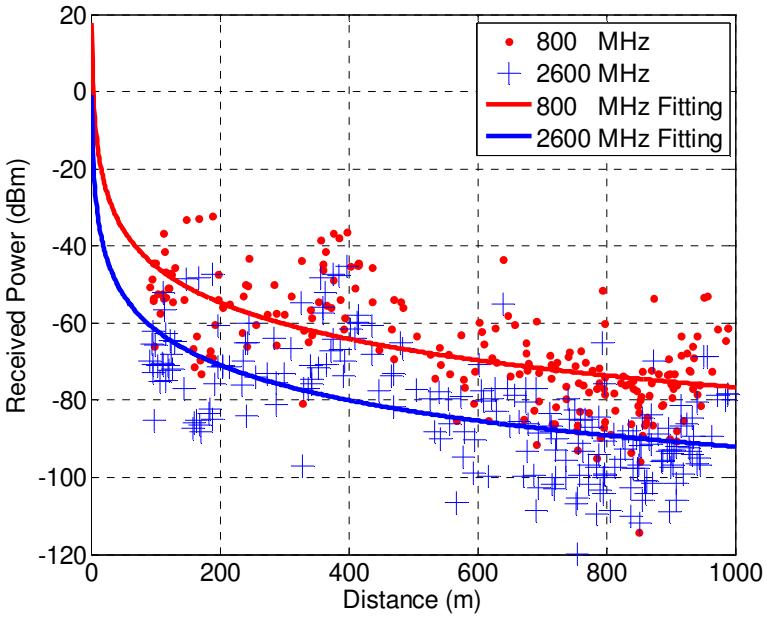

Figure-5: Total received signal strength (at the users) and best fit models as a function of distance from the base station at 800 MHz and 2.6 GHz

Simulation Results

This section presents the simulation results for single antenna systems using the LTE-Advanced link level Matlab simulator. In all cases a packet size of 300 Bytes is assumed. Figure-6 shows the Bit Error Rate (BER) vs SNR performance for the six scenarios in Table-3. From Table-3 it is clear that the K-factor is higher in the 800 MHz scenarios and the reduced fading then results in enhanced BER vs SNR performance. Figure-7(a) and Figure-7(b) show the PER versus SNR graphs for scenarios S1a and S1b respectively using different modulation and coding schemes. The results confirm that better performance is obtained in the 800 MHz band. The (1/2) and (3/4) code are obtained from the (1/3) code rate using the rate matching approach described in [12]. The corresponding throughput versus SNR graphs are shown in Figure-8(a) and Figure-8(b) respectively.

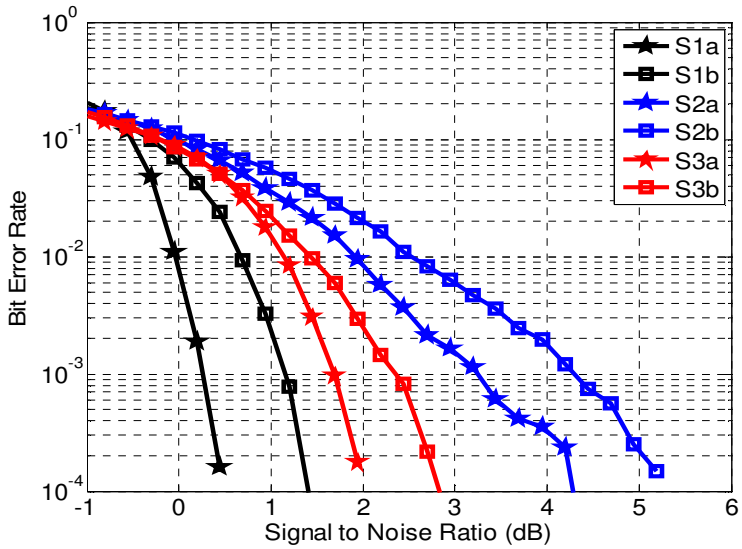

Figure- 6: BER v SNR for different scenarios [SISO, QPSK, TC (1/3), MMSE FDE, Packet size=300 Byte].

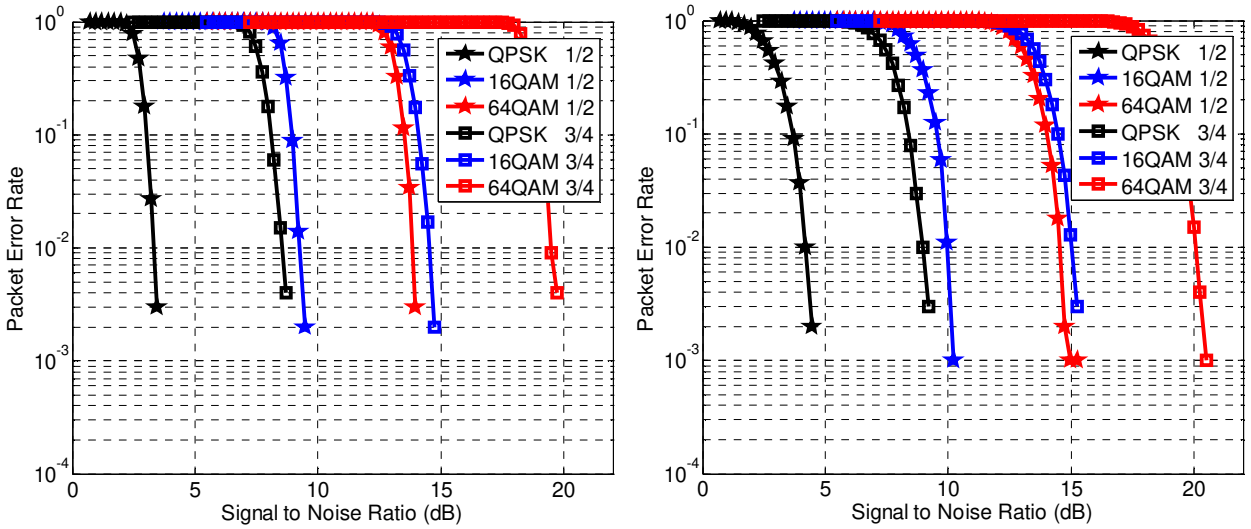

(a) (b)

Figure -7: PER v SNR for different Modulation and Coding Schemes [SISO, MMSE FDE, Packet size=300 Byte]; (a) Scenario S1a, (b) Scenario S1b

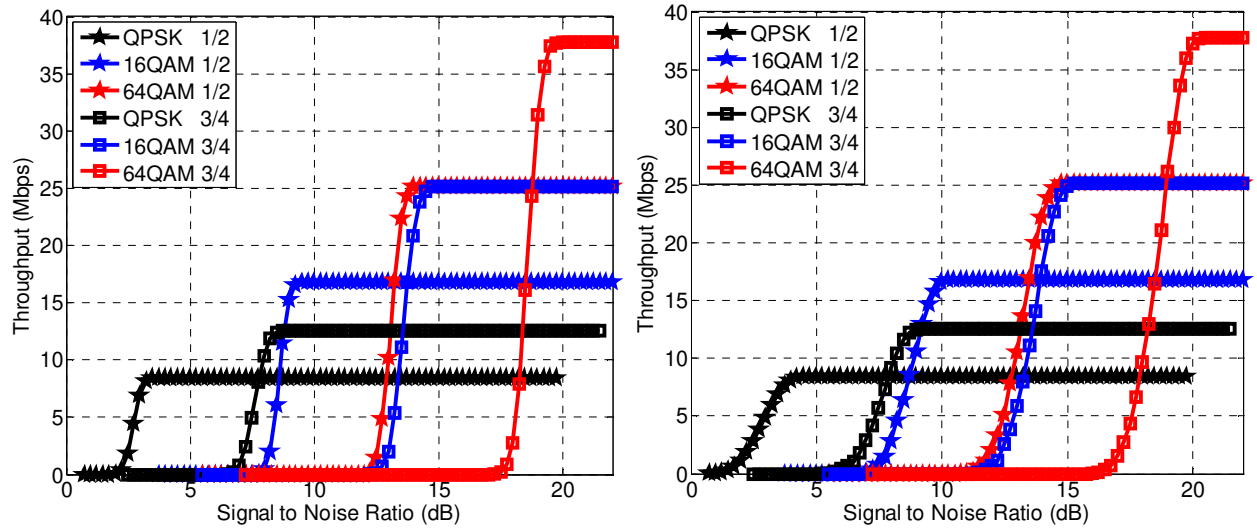

(a) (b)

Figure -8: Throughput v SNR for different modulation and coding Schemes [SISO, MMSE FDE, Packet size=300 Byte] (a) Scenario S1a, (b) Scenario S1b

To study the effect of the different frequency bands on the coverage, the average SNR at the UE with respect to BS separation distance was calculated and mapped to the throughput graphs of Figure-8 to obtain the throughput versus distance (Figure-9) for both frequency bands. The average SNR at each UE with respect to distance was calculated using (1)***[13]***:

$$(SNR)_{dB} = (P_{RX})_{dBm} - (K \times T \times B)_{dBm} - (F_{UE})_{dB} \quad (1)$$

where P_{RX} represents the average received power at the UE as obtained from the best fit model shown in Figure-5, K is Boltzmann's constant, T is the temperature, B is the effective bandwidth (calculated by multiplying the occupied subcarriers by the subcarrier spacing), and F_{UE} is the noise figure at the UE. For an LTE-Advanced UE, T=15ºC and F_{UE}=9 dB [14].

It is clear from Figure-9 that for distances up to 250 meters both bands achieve the same (maximum) throughput. The throughput performance in the 2.6 GHz band begins to degrade with distance beyond this point, dropping to 16.8 Mbps at a distance of 500 m. In the 800 MHz band, a maximum throughput of 37.8 Mbps is achieved up to 900 m. At this distance, the 2.6 GHz band offers a throughput of 8.4 Mbps only,

which is 4.5 times lower than the 800 MHz band. At a distance of 1.2 km, the 800 MHz band is still able to provide a 25 Mbps throughput while the 2.6 GHz band no longer provides coverage as can be seen in table-4.

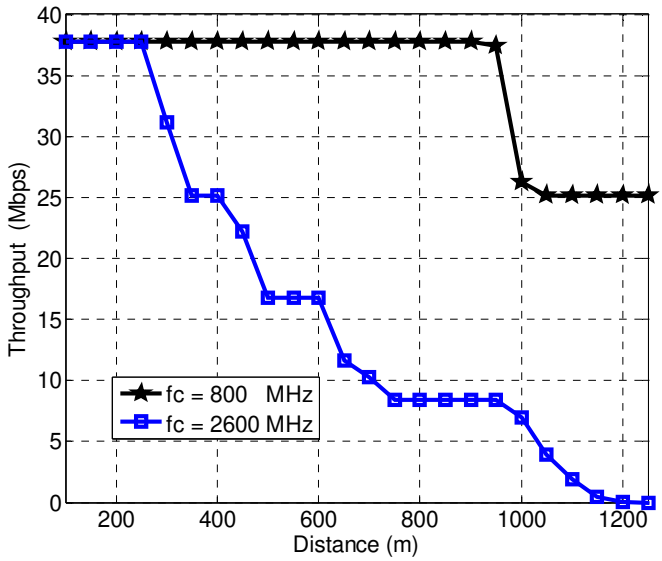

Figure -9: Throughput v Distance for the two frequency band [SISO, MMSE FDE, Packet size=300 Byte]

Table-4: Throughput at Different Distances

Distance (m)	**Throughput (Mbps)**	
	fc=800 MHz	**fc=2600 MHz**
250	37.8	37.8
500	37.8	16.8.
750	37.8	8.4
1000	25	7
1250	25	0

Conclusions

This paper has presented through simulation BER, PER and throughput performance analysis for the LTE-Advanced physical layer downlink channel using enhanced 3D ITU-R channel model at two different frequency bands. Better BER and PER performance was observed in the 800 MHz band due to reduced multipath (higher K-factor). The throughput of the two bands was computed as a function of BS-UE separation distance. Both bands offer maximum throughput performance up to 250 m, with the 800 MHz band maintaining this value up to 900 m.

From the results the following conclusion can be drawn. Carrier aggregation based on the two bands under study can be used at low BS-UE separation distances to increase capacity. The 800 MHz band is more suited to higher mobility users (such as vehicles), where the larger cell radius can reduce the number of handovers. Received powers in the 2.6 GHz band falls off faster with distance, and hence reduced interference would be observed in neighboring co-channel cells. As such, the 2.6 GHz band is better suited to supporting picocells in a HetNet scenario.

References

[1] Dahlman, S., and Skold, J.*"4G LTE/LTE-Advanced for Mobile Broadband,"* Oxford: Elsevier/Academic Press, (2011).

[2] Bugeja, M. *"Physical Layer Performance of LTE System with Multiple Antennas*," MSc, Department of Electrical and Electronic Engineering, University of Bristol, Bristol, United Kingdom, (2009).

[3] 3GPP TR 36.850. "*Evolved Universal Terrestrial Radio Access (E−UTRA): Inter-band Carrier Aggregation,*" V11.0.0, March (2013).

[4] Xiaoyi, Z., Doufexi, A., and Kocak, T. "*Throughput and Coverage Performance for IEEE 802.11ad Millimeter-Wave WPANs,*" IEEE Vehicular Technology Conference (VTC Spring), May (2011).

[5] Saeed, R., and Shellhammer, S. "*TV white space spectrum technologies: regulations, standards, and applications,*" Boca Raton, FL: CRC Press, (2012).

[6] Ameen, A. "*Physical Layer Enhancements for LTE-Advanced for 4G and Beyond Wireless Networks*," PhD Dissertation, Department of Electrical and Electronic Engineering, University of Bristol, United Kingdom, (2015).

[7] 3GPP TS 36.101. "*Evolved Universal Terrestrial Radio Access (E-UTRA); User Equipment (UE) radio transmission and reception (Release10)*", V10.6.0, March (2012).

[8] Almesaeed, R., Ameen, A., Doufexi, A., Dahnoun, N., and Nix, A. "*A Comparison Study of 2D and 3D ITU Channel Model*," IEEE Wireless Days, Valencia, Spain, November (2013).

[9] Almesaeed, R., Ameen, A., Mellios, E., Doufexi, A., and Nix, A. "*3D Channel Models: Principles, Characteristics, and System Implications,*" IEEE Communications Magazine, Vol. 55, No. 4, pp. 152-159, (2017).

[10] ITU-R M.2135-1. "*Guidelines for evaluation of radio interface technologies for IMT-Advanced*", December (2009).

[11] Enhanced 3D ITU channel model source code: http://enhanced-3d-itu-channel-model.sourceforge.net

[12] 3GPP TS 36.212: "*Evolved Universal Terrestrial Radio Access (E-UTRA); Multiplexing and channel coding (Release10)*", V10.5.0, March (2012).

[13] Doufexi, A., Tameh, E., Nix, A., Armour, S., and Molina, A.: "*Hotspot wireless LANs to enhance the performance of 3G and beyond cellular networks,*" IEEE Communications Magazine, Vol.41, No.7, pp. 58-65, (2003).

[14] 3GPP TS 36.942. "*Evolved Universal Terrestrial Radio Access (E-UTRA): Radio Frequency (RF) system scenarios*", V10.2.0, December (2010).